第33卷第5期
2014年10月

红外与毫米波学报
J. Infrared Millim. Waves

Vol. 33, No. 5
October, 2014

文章编号:1001-9014(2014)05-0460-05

DOI:10.3724/SP.J.1010.2014.00460

Influence of Mg doping on dielectric properties of ZnO nanopowders at terahertz frequencies

YUE Zhong-Yue[1], JIN Zuan-Ming[1], LI Gao-Fang[1], MA Guo-Hong[1*], MAO Zhi-Yong[2], ZHU Ying-Chun[2]

(1. Department of Physics, Shanghai University, Shanghai 200444, China;
2. Shanghai Institute of Ceramics, Chinese Academy of Sciences, Shanghai 200050, China)

Abstract: Transmitted terahertz time-domain spectroscopy (THz-TDS) using dipole-antenna on LT-GaAs was applied to determine the THz spectral characteristics of single-crystal ZnO, pure-and Mg-doped ZnO nanopowders (NPs) at room temperature. The power absorption and refractive index were measured in the frequency range from 0.2 to 2 THz. Mg doping increases the absorption coefficient, while decreases the refractive index of the compound ZnO NPs. The THz dielectric properties of pure-and Mg-doped ZnO NPs exhibit similar behaviors with that of the ZnO single crystal, which are found to be associated with the transverse optical E_1(TO) phonon mode.

Key words: terahertz time-domain spectroscopy, doping, complex dielectric constant, ZnO nanostructure
PACS: 42.70.Km

太赫兹频率下镁掺杂对氧化锌纳米粉体介电性能的影响

岳中岳[1], 金钻明[1], 李高芳[1], 马国宏[1*], 毛智勇[2], 祝迎春[2]
(1. 上海大学物理系,上海 200444;
2. 中国科学院上海硅酸盐研究所,上海 200050)

摘要:利用偶极天线LT-GaAs发射的太赫兹时域光谱(THz-TDS)研究单晶氧化锌、未掺杂和Mg掺杂的ZnO纳米粉末(粒子)在室温下的太赫兹光谱特性。在0.2~2 THz频率范围内研究了样品的功率吸收和折射率。结果发现,镁掺杂提高了样品材料的吸收效率,同时降低了氧化锌材料的折射率。相比较氧化锌单晶,未掺杂和Mg掺杂氧化锌纳米颗粒的太赫兹介电性质呈现类似的行为,该结果与横向光学E_1(TO)声子模式有关。

关 键 词:太赫兹时域光谱技术;掺杂;复介电常数;氧化锌纳米结构

中图分类号:O437 **文献标识码**:A

Introduction

Zinc oxide (ZnO) is one of the most intensively studied II-VI metal-oxide semiconductor with a direct band gap of 3.37 eV and a large exciton binding energy of 60 meV at room temperature, which has attracted enormous attention because of potential applications in photonic devices in ultraviolet range and spintronic devices in the past decade [1,2]. Recently, more and more interests are focus on the nanostructural ZnO materials, owing to the potential applications for nanodevice and nanotechnology [3,4], such as piezoelectric transduction, optical emission, drug delivery and optical storage. On the other hand, ZnO possesses a lot of advantages in terms of device applications in terahertz frequency range, for example ease in fabrication, wide band gap, high mobility, and transparency [5-8].

Owing to various morphologies, ZnO nanostructures exhibit quite different dielectric characteristics in THz range [9,10]. Besides morphologies, many factors dominate the optical properties of ZnO nanostructures as well, such as sample preparation conditions, host environment, defects, density-dependent properties and doping

Received date: 2013-05-27, **revised date**: 2013-09-10 **收稿日期**:2013-05-27, **修回日期**:2013-09-10
Foundation items: Supported by National Natural Science Foundation of China(11174195), Research Fund for the Doctoral Program of Higher Education of China(20123108110003)
Biography: YUE Zhong-Yue(1979-), male, Shangdong, Ph D. Research area involves terahertz wave generation and coherent control, optical coherent manipulation of electron spin. E-mail: yuezhongyue@shu.edu.cn
* **Corresponding author**: E-mail: ghma@staff.shu.edu.cn

condition so on. Especially, impurity doping has been used to enhance the electron emission (FE) efficiency and to tailor the optical properties[11,12]. It is essential to explore the dielectric properties of doped ZnO nanopowders (NPs) in the terahertz region.

In this paper, we report the far-infrared optical properties of ZnO single crystal, pure-and Mg-doped ZnO NPs (ZnO : Mg), characterized by normal transmitted THz time-domain spectroscopy (THz-TDS), advanced noncontact analyzing tools for complex dielectric properties in material science. The measured refractive index and power absorption coefficient were fit by classical pseudo-harmonic phonon model. It was demonstrated that Mg doping increases the absorption coefficient while decreases the refractive index of ZnO NPs in the THz range. The mechanism for THz dielectric response of ZnO : Mg NPs is similar to that in pure ZnO NPs and the single crystal, which is mainly dominated by the interaction of incident THz with lattice vibrations.

1 Experiments

The ZnO nanostructures were synthesized through thermal evaporation of ZnO powder in a horizontal high-temperature resistance furnace. The process was carried out at 1 250 °C under a flow of high-purity N_2 as a carrier gas. After the furnace was cooled to room temperature, powder of ZnO nanostructures with light yellow color were collected from the inner wall of the quartz tube. The fabrication of Mg-doped ZnO nanostructure began with the mixture powder of ZnO and MgO with ratio of 1 : 1 as the precursor in the furnace. The final atomic ratio between Mg and Zn in Mg : ZnO powder is about 5% ~ 8 % depending upon the position of quartz tube. The ZnO nanopowders are pressed in tablets with a diameter of 12 mm at a monometer pressure of no less than 2 MP using a hydraulic pressure. The thickness of pure and Mg-doped ZnO NPs tablets is 1.05 mm, and the thickness of ZnO single crystal is 0.52 mm.

The crystal structure and morphology of the ZnO NPs and Mg-doped ZnO NPs were characterized by high resolution X-ray diffraction (XRD) and scanning electron microscopy (SEM). The XRD and SEM patterns of ZnO NPs and Mg-doped ZnO NPs are shown in Fig. 1 (a) and (b), respectively. The hexagonal ZnO structure is obtained from the diffraction peaks with 2θ = 31.77°, 34.42°, 36.26°, 47.54° and 56.60°, respectively. The strongest peak appearing at 36.26° corresponds to (002) orientation of ZnO crystal, which indicates that the nanopowders grew predominantly along (002) direction. According to the XRD and SEM analysis, magnesium-doped-ZnO NPs show a similar structure as that of intrinsic ZnO. In addition, these two ZnO NP have the same porosity. The filling factor f, defined as the volume fraction of pure nanostructures and depended on the pressure applied, is used to evaluate the porosity of the NPs. The factor f is measured to be about 0.73 in current experiment.

For the terahertz time-domain measurement, a standard THz-TDS in transmission geometry was used to characterize the samples in the frequency range from 0.1 to 2.0 THz [13,14]. Briefly, the output of a mode-locked

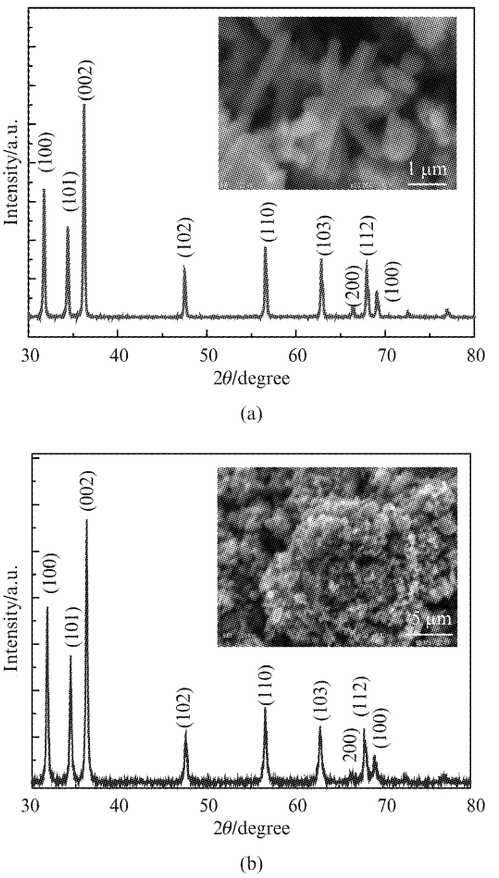

Fig. 1 (color online) XRD data of (a) ZnO NPs and (b) Mg-doped ZnO NPs. SEM images of ZnO NPs and Mg-doped ZnO NPs are shown in the inset

图 1 (a) ZnO 纳米粉末, (b) Mg 掺杂 ZnO 纳米粉末的 XRD 与 SEM 数据

Ti: sapphire laser, with pulse duration of 100 fs, centered wavelength at 800 nm, and repetition rate of 80 MHz (MaiTai HP, Spectra-Physics), is used to generate and detect the terahertz transient. The generated terahertz pulses are collimated into parallel beams by a microsilicon lens. A polyethylene lens is used to focus the terahertz beam on the sample position with a spot size of ~ 6 mm, the transmitted terahertz beams collimated with another polyethylene lens, and the final terahertz beams are collected by another silicon lens connected with a terahertz detector antenna. The sample is positioned at the beam waist of the THz beam. By a variable optical delay, the terahertz pulses generated at the emitter can be continuously delayed with respect to the gated detector, which allows us to temporally scan their electric field with both the amplitude and phase information. The THz-TDS system is purged with dry-N_2 gas to reduce THz absorption due to residual water vapor in the beam path.

2 Results and discussion

The THz pulses transmitted through pure ZnO NPs and ZnO : Mg NPs with their corresponding fast Fourier transformed (FFT) spectra are shown in Fig. 2 (a) and

(b). Due to the limited thickness of the ZnO NPs tablets, the main transmitted THz pulse (at ~ 13 ps) is trailed by multiple-reflected pulses in time domain. The propagation delay of THz pulse in time domain (with phase shift) is determined by the optical thickness of the sample. The refractive index can be obtained by measuring the physical thickness of the sample accurately. The damping of the electric field of THz pulse indicates the effective absorption during the propagation.

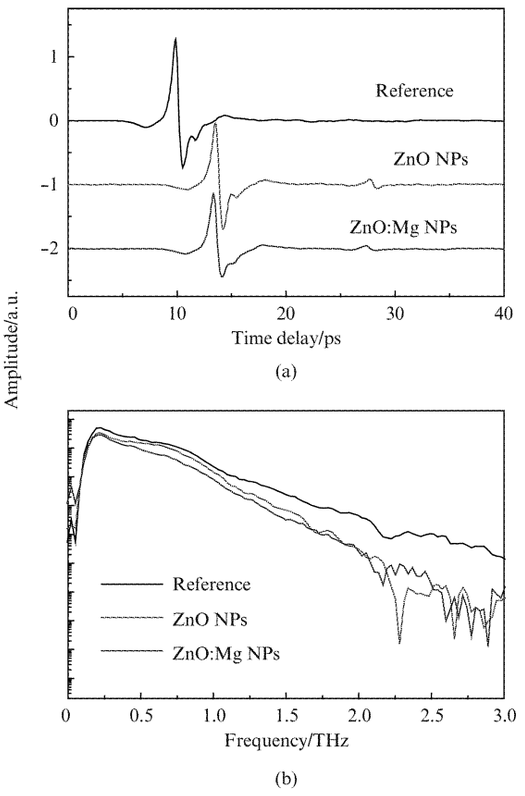

Fig. 2 (color online) (a) Measured THz pulses transmitted reference, pure ZnO NPs and ZnO : Mg NPs, which are vertically displaced for clarity. (b) Corresponding fast Fourier transformed spectra of the measured reference and sample pulses.
图2 (a) ZnO、Mg 掺杂 ZnO 纳米粉末与参考光的 THz 时域谱,(b) ZnO、Mg 掺杂 ZnO 纳米粉末与参考光傅里叶变换的频域谱

The complex refractive for nonmagnetic materials is written by $\tilde{n}(\omega) = \sqrt{\varepsilon(\omega)} = n(\omega) - i\kappa(\omega)$. The frequency dependent refractive index $n(\omega)$ and absorption coefficient $\alpha(\omega)$ can be directly obtained by the Fourier analysis of input THz pulse $E_{ref}(\omega)$ and output THz pulse $E_{sam}(\omega)$ [6,13]:

$$n(\omega) = 1 + \frac{c\phi(\omega)}{\omega d}$$
$$\alpha(\omega) = 2\frac{\omega}{c}\kappa(\omega) = -\frac{2}{d}\ln\left\{\frac{[n(\omega)+1]^2}{4n(\omega)}T(\omega)\right\} \quad ,(1)$$

where d is the thickness of sample, c is the speed of light in vacuum. $T(\omega)$ and $\phi(\omega)$ are defined as $T(\omega)e^{i\phi(\omega)} = \frac{4n(\omega)}{[n(\omega)+1]^2}e^{-\frac{\alpha d}{2}}e^{i\left(\frac{\omega}{c}\right)d[n(\omega)-1]}$.

The frequency-dependent dielectric response $\varepsilon(\omega)$ is described by $\varepsilon(\omega) = \varepsilon_r(\omega) - i\varepsilon_i(\omega) = [n(\omega) - i\kappa(\omega)]^2$, where the imaginary part of the refractive index $\kappa(\omega) = \alpha(\omega)\lambda_0/4\pi$. The measured samples are composites of nanostructures and air. The effective dielectric function can be treated by simple effective medium theory (EMT), $\varepsilon_{eff} = f\varepsilon_m(\omega) + (1-f)\varepsilon_h(\omega)$ [9], where $\varepsilon_m(\omega)$ is the dielectric function of pure-ZnO NPs, $\varepsilon_h(\omega)$ is dielectric constant of the host medium, giving $\varepsilon_h = 1$ for air in the present study. The filling factor $f = 0.73$ is measured in the experiment. ε_{eff} is the measured effective dielectric constant of the composite material, which includes nanostructures and air.

In Figs. 3 (a) ~ (c), we present THz-TDS results, the refractive index and absorption coefficients, on Mg-doped, pure-ZnO NPs and single crystal ZnO. The refractive index is nearly constant of 2.33 and 2.27 for pure ZnO NPs and ZnO : Mg NPs, respectively, much less than 2.84 for single-crystal ZnO. In addition, the pure-and Mg-doped ZnO NPs have similar absorption behaviors, in comparison with that of the single-crystal ZnO, which increases with frequency. It can be found that the absorption coefficient of ZnO : Mg NPs is slightly larger than that of ZnO NPs at the frequency range of 0.40 ~ 1.70 THz, as shown in Fig. 3 (d). No prominent absorption peak is observed below 2.0 THz.

The dielectric constant $\varepsilon_m(\omega)$ can be represented by [14]:

$$\varepsilon_m(\omega) = \varepsilon_\infty - \frac{\omega_p^2}{\omega^2 + i\gamma\omega} + \sum_j \frac{\varepsilon_{st}\omega_{TO_j}^2}{\omega_{TO_j}^2 - \omega^2 - i\Gamma_j\omega} \quad ,(2)$$

where ε_∞ is the high-frequency dielectric constant, the second term describes the contribution of free electrons (*Drude response*), and the third term is due to the contribution of optical phonons (*Lorentzian oscillator*). The plasma frequency ω_p and the carrier damping constant γ describe the dynamics of free electrons or plasmons in semiconductors. $\omega_p = \left(\frac{Ne^2}{\varepsilon_0 m^*}\right)^{\frac{1}{2}}$, where N is the carrier density, m^* is the effective mass of the electron, and ε_0 is the free-space permittivity. In addition, the mobility can be obtained by $\mu = \frac{e}{\gamma m^*}$. The summation term in Eq. (2) is over all lattice oscillations with the jth transverse optical (TO) frequency ω_{TOj}, oscillator strength ε_{stj}, and phonon damping constant Γ_j. ε_{st} is connected to the high-frequency dielectric constant ε_∞ and background dielectric constant $\varepsilon(0)$ by $\varepsilon_{st} = \varepsilon(0) - \varepsilon_\infty$. By comparing the fitting results with different models, we found that the dielectric responses of ZnO NPs and bulk ZnO single crystal are mainly attributed to lattice vibrations, which is described well theoretically by the classical pseudo-harmonic phonon model. The main dielectric response is from phonon vibrational mode, and then $\varepsilon_m(\omega)$ of Eq. (2) with the first approximation can be simplified as: $\varepsilon_m(\omega) = \varepsilon_\infty + \frac{\varepsilon_{st}\omega_{TO}^2}{\omega_{TO}^2 - \omega^2 - i\Gamma\omega}$. The fit on the classical pseudo-harmonic phonon model, shown by the solid curves in Fig. 3, indicating that the absorption

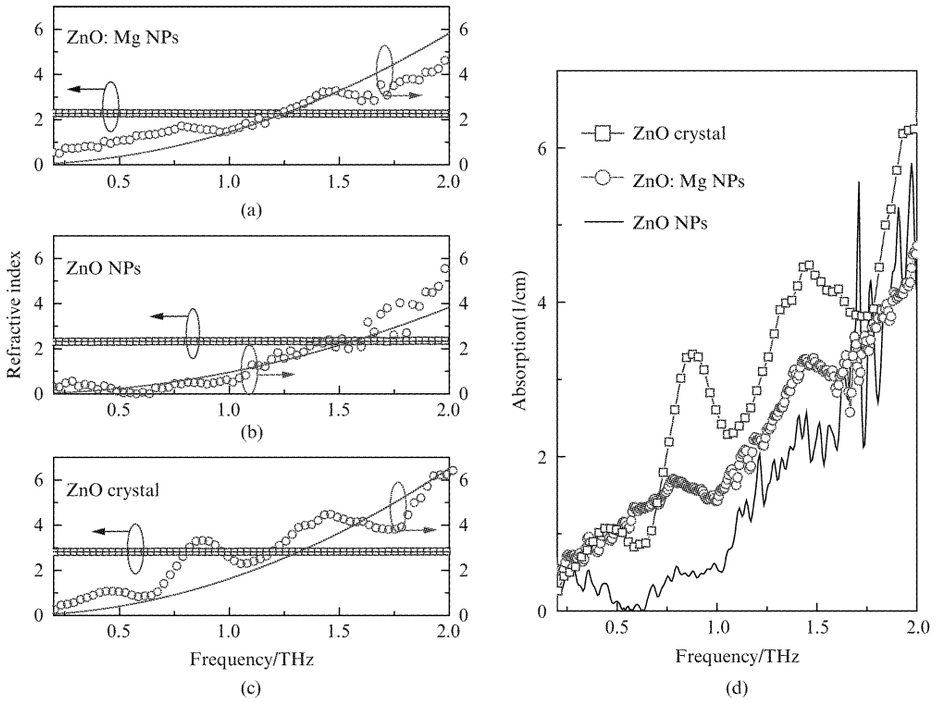

Fig. 3 (color online) Refractive indices and absorption coefficients of (a) Mg-doped ZnO NPs, (b) pure ZnO NPs, and (c) single-crystal ZnO with theoretical fitting, respectively. (d) The absorption coefficients of three samples for comparison

图 3 (a)(b)(c)分别是 Mg 掺杂 ZnO 纳米粉末，ZnO 纳米粉末与 ZnO 单晶的折射率与吸收系数。(d)三个样品吸收系数的比较

of ZnO NPs and ZnO single crystal are dominated by the transverse optical mode localized at $\omega_{TO}/2\pi$ = 12.42 THz, a typical transverse optical mode in the bulk ZnO of wurtzite structure with the assignment E_1(TO), with different parameters: $\Gamma/2\pi = 3.0$ THz, $\varepsilon_\infty = 2$, $\varepsilon_{st} = 3.45$; $\Gamma/2\pi = 4.5$ THz, $\varepsilon_\infty = 1.75$, $\varepsilon_{st} = 3.4$; and $\Gamma/2\pi = 5.0$ THz, $\varepsilon_\infty = 3.7$, $\varepsilon_{st} = 4.2$ for pure-ZnO NPs, Mg-doped ZnO NPs, and ZnO single crystal, respectively.

It is seen from Fig. 3 that the refractive indices for both pure ZnO and doped ZnO NPs are much less than that of ZnO single crystal. By comparing with the pure-ZnO NPs, the refraction index of Mg-doped sample slightly decreases about 0.06. This difference could be related to the poor crystallization of the ZnO NPs after doping. The different crystallization in pure ZnO and Mg-doped ZnO NPs can be seen more pronounced from the THz power absorption spectra. Although ZnO and Mg-doped ZnO NPs are fabricated under similar condition, the dopant such as Mg is expected to affect the crystallinity of the ZnO NPs. The SEM images reveal that crystallization and morphology in pure ZnO NPs is quite different from that of Mg-doped ZnO NPs (Figure 1). Therefore, it is reasonable to infer that the different dielectric constants in pure ZnO NPs, doped ZnO NPs and ZnO single crystal are associated with the crystallization and morphology. The morphology difference may cause different degrees of crystallization as proved by SEM images. Different crystallization in these powders could lead to different densities of structure defects, which in turn result in different carrier concentrations. Owing to that the real conductivity is proportional to the imaginary part of dielectric constant, $\sigma_1 = \omega\varepsilon_i\varepsilon_0$, Mg doping is expected to increase the conductivity of ZnO NPs due to the poor crystallization.

It should be mentioned that doping in semiconductor may also lead to increase the electron or hole concentration in the host semiconductor, such as in gallium-doped ZnO : Ga nanofiber. However, different doping effect has been observed in CeO_2, the absorption coefficient of Fe-doped CeO_2 is less than undoped CeO_2 at 0.2 to 1.8 THz [14]. These results suggest that the feasibility of doping for tailoring the optical properties of oxide semiconductors at THz frequencies. As for the case of Mg-doped ZnO NPs, there are no free carriers available from the dopants, the only reason for enhancing conductivity by doping comes from the crystallization changes after dopant, Mg, is introduced in ZnO NPs.

3 Conclusions

In summary, we have studied the far-infrared dielectric properties of single-crystal ZnO, pure-and Mg-doped ZnO NPs. The THz-TDS data for power absorption and refractive index of the nanopowders samples are well fit by phonon model combined with the simple effective medium theories. Our THz-TDS characterization implicates that the dielectric response of ZnO NPs, similar to

that in bulk single-crystal ZnO, is related to the E_1(TO) phonon mode at 12.42 THz. Mg doping effectively reduces the crystallization of ZnO NPs, and the absorption coefficient of the doped ZnO NPs is increased in the THz range due to more structure defects with doping.

Acknowledgement

The research is supported by National Natural Science Foundation of China (11174195), and Ph. D. Programs Foundation of Ministry of Education of China (20123108110003).

References

[1] Özgür Ü, Alivov Y I, Liu C, *et al*. A comprehensive review of ZnO materials and devices[J]. *J. Appl. Phys*. 2005, **98**: 041301-1-041301-103.

[2] Klingshirn C. ZnO: From basics towards applications[J]. *phys. stat. sol*. (b), 2007, **244**: 3027-3073.

[3] Wang Z L Novel nanostructures of ZnO for nanoscale photonics, optoelectronics, piezoelectricity, and sensing[J]. *Appl. Phys. A* 2007, **88**: 7-15.

[4] Tian Z R, Voigt J A, Liu J, *et al*. Complex and oriented ZnO nanostructures[J]. *Nature Mater*. 2003, **2**: 821-826.

[5] Azad A K, Han J, Zhang W. Terahertz dielectric properties of high-resistivity single-crystal ZnO [J]. *Appl. Phys. Lett*. 2006, **88**: 021103-1-021103-3.

[6] Ma G H, Li D, Ma H, *et al*. Carrier concentration dependence of terahertz transmission on conducting ZnO films[J]. *Appl. Phys. Lett*. 2008, **93**: 211101-1-211101-3.

[7] Kim Y, Ahn J, Kim B G, *et al*. Terahertz Birefringence in Zinc Oxide [J]. *Jpn. J. Appl*. Phys. 2011, **50**: 030203-1-030203-3.

[8] Baxter J B, Schmuttenmaer C A, Carrier dynamics in bulk ZnO. I. Intrinsic conductivity measured by terahertz time-domain spectroscopy [J]. *Phys. Rev. B* 2009, **80**: 235205-1-235205-6.

[9] Han J G, Zhang W, Chen W, *et al*. Terahertz Dielectric Properties and Low-Frequency Phonon Resonances of ZnO Nanostructures[J]. *J. Phys. Chem. C* 2007, **111**: 13000-13006.

[10] Balci S, Baughman W, Wilbert D S, *et al*. Characteristics of THz carrier dynamics in GaN thin film and ZnO nanowires by temperature dependent terahertz time domain spectroscopy measurement[J]. *Solid-State Electron*. 2012, **78**: 68-74.

[11] Xu C X, Sun X W, Chen J B. Field emission from gallium-doped zinc oxide nanofiber array[J]. *Appl. Phys. Lett*. 2004, **84**: 1540-1542.

[12] Jung M N, Ha S H, Oh S J, *et al*. Field emission properties of indium-doped ZnO tetrapods[J]. *Curr. Appl. Phys*. 2009, 9,: e169-e172.

[13] Ulbricht R, Hendry E, Shan J, *et al*. Carrier dynamics in semiconductors studied with time-resolved terahertz specrtoscopy [J]. *Rev. Mod. Phys*. 2011, **83**: 543-586.

[14] Wen Q, Zhang H, Yang Q, *et al*. Fe-Doped Polycrystalline CeO_2 as Terahertz Optical Material[J]. *Chin. Phys. Lett*. 2009, **26**: 047803-1-047803-4.